

SURFACE-ACOUSTIC-WAVE DEVICE FOR DOPPLER FILTERING OF RADAR BURST WAVEFORMS*

J. Melngailis and R. C. Williamson
Lincoln Laboratory, Massachusetts Institute of Technology
Lexington, Massachusetts 02173

ABSTRACT

A new type of reflective-grating matched filter has been developed for processing a Doppler-sensitive burst waveform consisting of 16 equally spaced phase-coherent linear-FM subpulses. The subpulses have 60-MHz bandwidth, are 3- μ s long, and have a period of 5 μ s. After addition of internal phase compensation, the phase response of the device over all 16 subpulses is within $\pm 20^\circ$ of ideal. When a burst waveform is compressed in this burst matched filter, the range (time) sidelobes are approximately -40 dB down except for some near-in at -33 dB, and the Doppler (velocity) sidelobes are -32 dB down.

INTRODUCTION

Range and velocity of radar targets can be simultaneously measured by using burst waveforms. One type of burst waveform consists of a train of coherent linear-FM subpulses¹. The range is determined by the arrival time of the reflected return, the velocity is determined by sensing the changes in subpulse-to-subpulse spacing produced by the Doppler shift. For example, a waveform reflected from an approaching target is contracted in time. One consequence of the use of a burst waveform is ambiguities in both range and Doppler¹. Often the ambiguities can be removed by subsequent processing. Existing analog techniques for matched filtering of burst waveforms are limited both in bandwidth and dynamic range. Alternate digital techniques often force an unattractive trade-off between bandwidth and range window. Wide-band processing with large dynamic range and infinite range window is the significant feature of the device described herein. We propose doing the signal processing with a bank of surface-acoustic-wave burst matched filters wherein each filter is matched to a different velocity². To demonstrate the feasibility of this new approach, we have built one such filter for processing an 80- μ s-long waveform with a bandwidth of 60 MHz. From previous experience^{3,4} we expect to be able to increase the bandwidth by at least a factor of 4. The surface wave device is likely to lead to a reduction in system complexity compared to the conventional approaches.

DEVICE CHARACTERISTICS

The burst matched filter consists of 16 reflective-array-compressor sections end to end on a 15.2-cm-long Y-Z LiNbO₃ crystal. The device is shown schematically in Fig. 1. The filter is matched to a burst radar waveform consisting of 16 phase-coherent linear-FM subpulses. The bandwidth of each subpulse is 60 MHz centered at 200 MHz, its length is 3 μ s, and the subpulse-to-subpulse period is 5 μ s. The time-bandwidth product of each subpulse is 180, and the overall time-bandwidth product is 4800.

The reflective arrays are ion-beam etched. The depth is varied so that each section is Hamming weighted for range sidelobe suppression. The relative response of successive sections is Hamming weighted for Doppler-sidelobe suppression. This is seen in the impulse response in Fig. 2. The frequency response of each of the individual sections is shown in Fig. 3. It also shows the Hamming-on-Hamming weighting.

In order to test the response of the burst matched filter, a burst waveform generator was also fabricated. To this end, a pulse expander was built to generate a subpulse of the burst waveform. The expander is identical to a single burst-matched-filter section except that the effective array is ion-beam etched so as to achieve a flat frequency response from 170 to 230 MHz instead of the Hamming function. When it is coherently impaled 16 times, a train of linear-FM subpulses results. Before processing in the burst matched filters

the sense of chirp in each subpulse is inverted by mixing with 400 MHz. The result of compressing the entire wave-train in a phase-compensated burst matched filter (see below) is shown in Fig. 4. The central, 16th, compressed pulse (out of a total of 31) is shown in Fig. 4(a). Relative to the main pulse the sidelobes are seen to be at the -40 dB level, except for some near-in sidelobes at -33 dB. Fig. 4(b) shows the peak of the compressed pulse in Fig. 4(a) as a function of the mixing frequency. This simulates the Doppler shift produced by reflection from a moving target. The Doppler resolution or width of the main response in Fig. 4(b) is 18 kHz which would provide a velocity resolution of 900 m/s in a 3 GHz radar. The distance between the peaks is 200 kHz, the inverse of 5 μ s. Figure 4(c) is the same as Fig. 4(b) except the vertical scale is expanded 10 times. The Doppler sidelobe level is at approximately -32 dB. Figures 4(a) and 4(b) are cuts along range and Doppler, respectively, of the ambiguity diagram for the combined waveform and processor.

PHASE RESPONSE

Because the operation of a burst matched filter depends on the coherent addition of 16 compressed pulses, the phase response of the device is very important. Ideally, the incremental delay τ' between sections should be constant, and each section should have the same linear chirp slope $\Delta T/\Delta f$. The ideal phase response is

$$\phi_{\text{ideal}} = 2\pi [\tau f + (n-1)\tau' f + \frac{\Delta T}{2\Delta f} (f - f_0)^2] \quad (1)$$

where τ is the delay to the first section, $n = 1, 2, \dots, 16$ refers to section number, and f_0 is the center frequency. Phase deviations from ideal reduce the correlation gain in the device and cause degraded range and Doppler sidelobes.

In a burst matched filter, phase errors can be reduced by first measuring the phase response and depositing an appropriately patterned phase-compensating metal film between the grating sections³, as shown in Fig. 1. The film provides a way of varying the delay for different parts of the waveform. Our first attempt at phase compensation is shown in Fig. 5. The phase deviations shown before and after phase compensation are the deviations from a best fit of the data to Eq. 1 wherein the parameters τ , τ' , and $\Delta T/\Delta f$ were varied for minimum deviations. Although significantly reduced, phase deviations still exist after the compensation pattern is fabricated. The near-ideal compressed-pulse performance shown in Fig. 4 was achieved in a device with the phase response of Fig. 5, but with a somewhat poorer amplitude response than that shown in Fig. 2 & 3. In principle, the phase-compensation process could be iterated to further reduce phase errors and achieve even better performance.

Several effects may contribute to the large $\pm 20^\circ$ phase errors observed before compensation: a) mask errors, b) slowing effect of grooves due to energy storage^{5,6} and c) surface-wave velocity variations on the crystal. Mask errors such as a displacement of one grating with respect to another may account for the jogs in the uncorrected curve in Fig. 5. A 20° jog would be

* This work is sponsored by the Department of the Army.

produced by a 0.5- μm displacement. The downward dip of the entire phase response curve at section 9 is also reproduced in the phase response of two other devices made with the same mask, but some other features are not.

Energy storage in grooves leads to a small phase shift of a surface wave transmitted past a step. Because the amount of phase shift is related to groove depth, the variations of groove depth within the ion-beam-etched arrays perturb the phase response of the device. Theoretical calculations of the magnitude of such phase errors indicate that energy storage effects contribute at most $\pm 25^\circ$ to the measured phase errors (curves A of Fig. 5).

Several qualitative observations suggest that velocity variations along the length of the crystal may be responsible for most of the initial phase errors. Such velocity variations may be caused by surface inhomogeneities or by internal stresses in the crystal. We have observed that the phase response of a device held down in a temporary package by screws varied by several tens of degrees as the screws were tightened and loosened. (All phase measurements reported were made with loose screws). After cutting and polishing of LiNbO_3 crystals they are usually slightly bowed indicating the presence of internal stresses. On all three burst matched filters made so far, annealing at 100°C for 10 to 20 hours reduced the overall spread of the phase error by as much as 100° . The velocity variation needed to explain the observed effects is very small: $\Delta v/v = 10^{-4}$ over the 5 μs delay between sections would lead to a phase deviation of 36° . More than ten-times-larger velocity variations from sample to sample have been measured⁷. Fortunately, the technique of phase compensation allows phase errors, no matter what the source, to be significantly reduced to achieve near-ideal matched-filter performance.

SUMMARY

The feasibility of using chirped-grating surface-wave devices for Doppler-sensitive radar processing has been demonstrated. As with previous reflective-array devices, good amplitude and phase response can be achieved. This results in the low range and Doppler sidelobes which are required for use in a radar.

ACKNOWLEDGEMENTS

The authors are indebted to N. Efremow, Muriel Dalomba, W. T. Brogan, W. C. Kernan, R. P. Konieczka and S. Cupoli for fabricating, assembling, and testing the device, and to J. Holtham for computer programming the measurements and the analysis.

REFERENCES

- 1) H. Urkowitz, "Resolution, ambiguity pulse compression techniques", *Modern Radar*, R. Berkowitz, ed., New York, Wiley (1965).
- 2) R.C. Williamson, J. Melngailis, and V.S. Dolat, "Reflective-Array matched filter for a 16-pulse radar burst", *1975 Ultrasonics Symposium Proceedings*, New York: IEEE, 1975, pp. 400-404.
- 3) R.C. Williamson, V.S. Dolat, and H.I. Smith, "L-band reflective-array compression with a compression ratio of 5120", *1973 Ultrasonics Symposium Proceedings*, New York: IEEE, 1973, pp. 490-493.
- 4) H.M. Gerard, O.W. Otto, and R.D. Weglein, "Development of a broadband reflective-array 10,000:1 pulse compression filter", *1974 Ultrasonics Symposium Proceedings*, New York: IEEE, 1974, pp. 197-201.
- 5) R.C.M. Li and J. Melngailis, "Influence of stored energy at step discontinuities on the behavior of surface-wave gratings", *IEEE Trans. Sonics Ultras.*, Vol. SU22, pp. 189-198, May, 1975.
- 6) J. Melngailis and R.C.M. Li, "Measurement of impedance mismatch and stored energy for right-angle reflection of Rayleigh waves from grooves on Y-cut LiNbO_3 ", *1975 Ultrasonics Symposium Proceedings*, New York: IEEE, 1975, pp. 426-429.
- 7) R.C. Williamson, "Measurement of the propagation characteristics of surface and bulk waves in LiNbO_3 ", *1972 Ultrasonics Symposium Proceedings*, IEEE Cat. # CHO 708-8SU, p. 323.

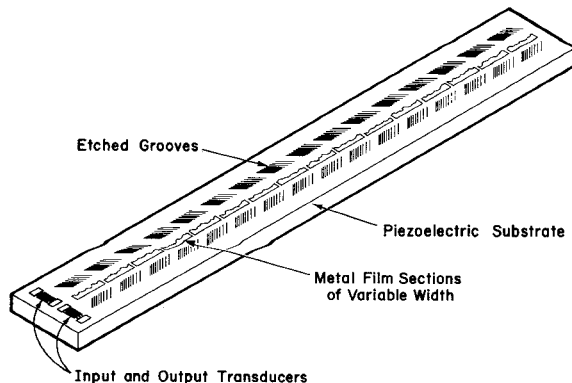


Fig. 1 Schematic of surface-acoustic-wave burst matched filter. The substrate is 15.2-cm-long Y-Z LiNbO_3 crystal. Phase-compensating metal film is shown deposited between the reflective arrays.

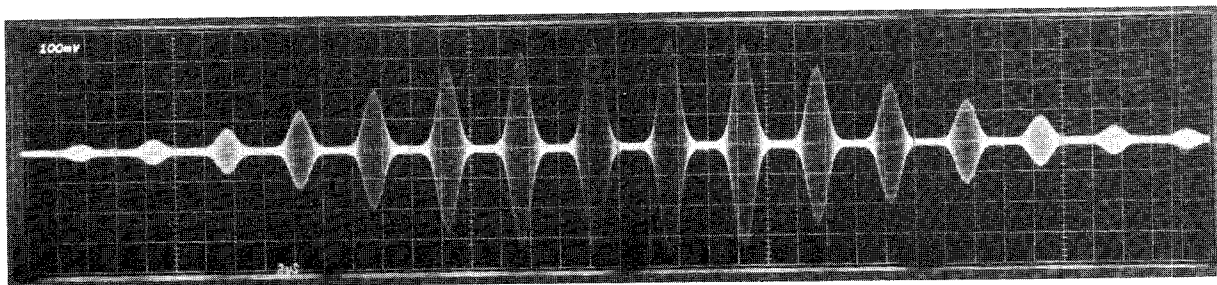


Fig. 2 Impulse response of the filter. Each section is Hamming weighted and the overall envelope is Hamming weighted. Horizontal scale is 2 μ s/div.

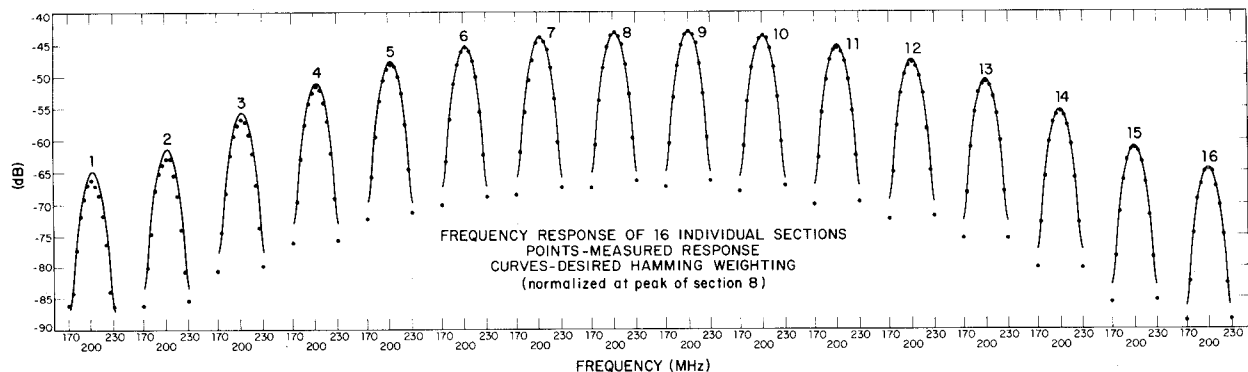


Fig. 3 Frequency response of the 16 individual sections. Solid curves are the desired Hamming-on-Hamming weighting. The calculated curves are normalized to the data points at the peak response in Section 8.

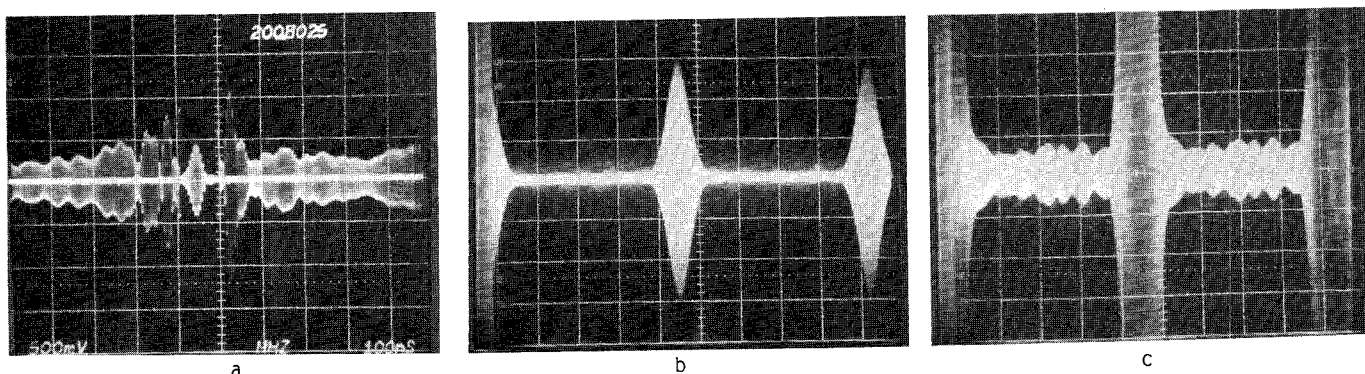


Fig. 4 (a) The central compressed pulse produced by inputting a 16-pulse wave train to the burst processor. Vertical scale 500 mV/div., expanded 5 mV/div. Horizontal scale 100 μ s/div. (b) The amplitude of the central compressed pulse vs. mixer frequency. This simulates Doppler shift. Horizontal scale 42 kHz/div. (c) Same as 4(b) expanded 10 times on the vertical scale.

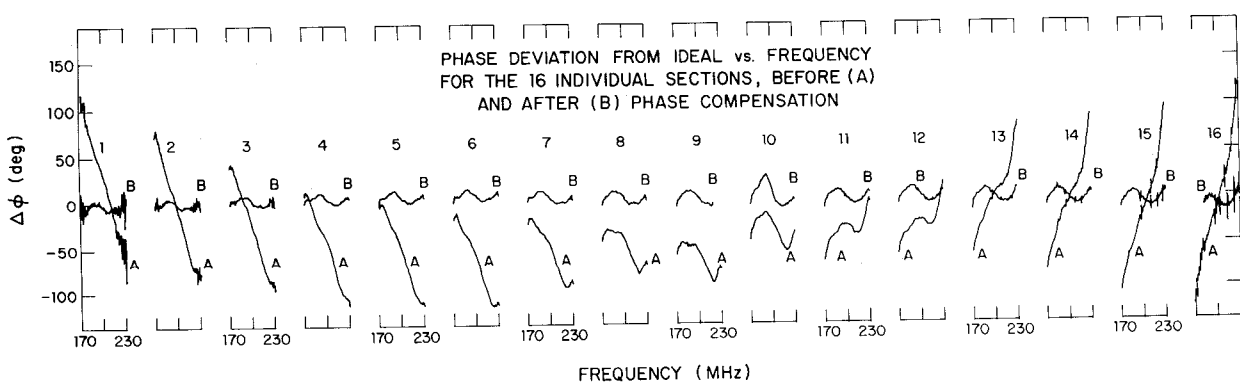


Fig. 5 Overall phase deviation from ideal, Eq. (1), for all 16 sections of the burst matched filter. The curves B show the phase deviation after a phase correcting metal film is deposited between the gratings, see Fig. 1.